ACS OMEGA

http://pubs.acs.org/journal/acsodf

Article

Impact of Ionic Liquid on Hydrogen Production from Waste Oilfield Water

Mohamed A. Deyab* and Ahmed E. Awadallah

Cite This: *ACS Omega* 2021, 6, 31964−31970

Read Online

ACCESS | Metrics & More | Article Recommendations

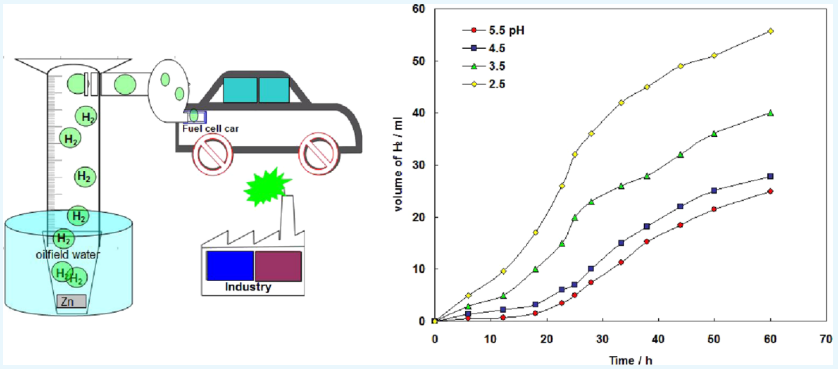

ABSTRACT: We present a promising method for producing pure hydrogen energy from the dissolution of zinc metal in waste oilfield water (WOW) under various conditions. This process mainly consumes zinc metal and WOW. The results show robust dependence on the temperature and solution pH of the hydrogen gas output. Low pH (2.5) and high temperature (338 K) were discovered to be the better conditions for hydrogen production. The 1-ethyl-3-methylpyridinium ethyl sulfate (EMP-ES) ionic liquid is used to regulate the rate of hydrogen generation for the first time. It has been confirmed that the rate of the dissolution of zinc increased faster and produced more hydrogen per unit of time by an increase in solution temperature and a decrease in solution pH. The adsorption of EMP-ES on the active sites of the Zn surface is unrestrained with mixing physical and chemical orientations. SEM, EDX, and FTIR spectroscopy inspections have been utilized to identify and characterize surface corrosion of zinc in WOW. Furthermore, this process is completely secure and can generate energy on demand.

1. INTRODUCTION

The search for modern energy sources has been a vital center of attention recently because of environmental pollution by fossil fuels. A variety of toxic air pollutants and carbon dioxide (CO_2) are among the hazardous pollutants. Hydrogen gas is a favorable energy source due to its high energy content and low environmental risk.[1−5] A hydrogen fuel cell in a vehicle emits no pollutants; the only things that escape by the engine exhaust are steam and heat. Hydrogen energy can be generated from various origins like water, ethanol, natural gas, and so forth. There is a persistent requirement to find renewable, cheap, and clean materials for hydrogen energy generation.

Latterly, the chemical dissolution of some metals accompanied by hydrogen generation became a promising method in the scope of hydrogen energy.[6] In these processes, the hydrogen gas sources like H_2O and hydrocarbons are commonly employed as one of the reactants, from which hydrogen gas will be drawn out with the help of metals.[7−10]

The on-demand hydrogen production by metal dissolution in suitable solutions can exclude the necessity for hydrogen storage.[11] Aluminum and its alloys have been used extensively for producing hydrogen energy. In 2009, Soler et al.[12] showed that hydrogen can be generated by corrosion of aluminum in aqueous solutions of sodium aluminate. They indicated that the solution pH plays a great role in the amount of hydrogen energy. They noted that the surface of aluminum becomes passive after some hours, and this affects the rate of hydrogen generation. By adding aluminate anions in the aqueous solution, they succeeded in preventing aluminum surface passivation. According to this data, it was clear that the passive layer that formed on the metal surface during hydrogen energy production considers the main problem facing this method. Deyab[10] used the lactic acid solution in the presence of perchlorate ions to improve the dissolution of tin metal and to

Received: August 30, 2021
Accepted: November 8, 2021
Published: November 17, 2021

prevent the formation of the passive film. He found that by adding perchlorate ions, much improvement in the hydrogen generation rate was obtained. Huang et al.[13] indicated that the incorporation of graphite with aluminum can significantly inhibit the formation of the passive layer and lead to the high yield of hydrogen at ordinary conditions.

Here, our new strategy to produce hydrogen energy depends on the metal dissolution (Zn) in waste oilfield water (WOW). By this strategy, we can decrease the cost of hydrogen energy production because we use waste materials from the petroleum field.[14] At the same time, this WOW contains highly corrosive chloride ions, and these ions prevent the formation of the passive layer in the metal surface.[15] This means that in this solution (i.e., WOW), the yield of hydrogen energy will be very large without adding any additives.

It is also very important to control the hydrogen generation reaction according to the production conditions. Organic compounds and surfactants were used in regulating hydrogen generation before this investigation. To manage hydrogen evolution in acidic solution, Sanatkumar et al.[16] used 2-(4-chlorophenyl)-2-oxoethyl benzoate. Deyab[9] discovered that some organic surfactants can be used effectively to monitor hydrogen evolution. For this objective, the new ionic liquid (1-ethyl-3-methylpyridinium ethyl sulfate) is used to regulate the rate of hydrogen generation. Also, this represents an additional novelty for this work.

2. RESULTS AND DISCUSSION

2.1. Hydrogen Gas Measurements. Figure 1 shows the volume of hydrogen gas evolution from the dissolution of zinc coupons placed in WOW (pH 5.5) with time at 298 K. The figure clearly shows that the rate of hydrogen gas output increases with increasing time.[17]

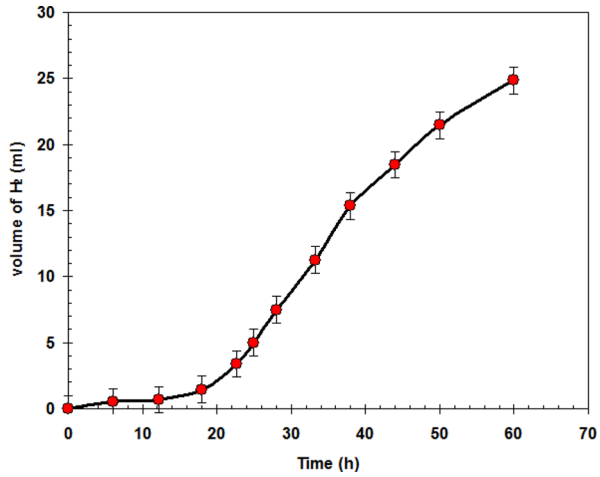

Figure 1. Variation of H_2 volume (mL) with time (h) during the dissolution of the Zn electrode in WOW (pH 5.5) at 298 K.

Zinc coupons are readily dissolved in WOW, resulting in hydrogen production. The anodic and cathodic reactions for the dissolution of zinc metal in WOW (pH 5.5) can be presented as the following[18]

(a) Anodic part

$$Zn \rightarrow Zn^{++} + 2e \quad (1)$$

(b) Cathodic part

$$2H^{+} + 2e \rightarrow H_{2(g)}\uparrow \quad (2)$$

The overall dissolution processes are epitomized in eq 3

$$Zn_{(s)} + 2H^{+} \rightarrow Zn^{++} + H_{2(g)}\uparrow \quad (3)$$

It is clear from the abovementioned reactions that the electrons are transferred from the anodic process (oxidation process) to the cathodic process (hydrogen gas evolution).[19] The anodic and cathodic processes should continue at the same time and at equivalent rates.[20]

SEM and EDX analysis have been utilized to identify and characterize surface corrosion. SEM observations for Zn metal before and after its immersion in WOW (Figure 2) confirm that the Zn surface is enveloped with high intensity of pits and corrosion products.

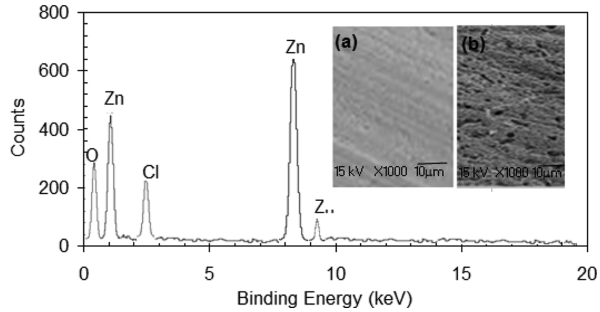

Figure 2. SEM observations of the Zn electrode surface before (a) and after (b) its immersion in WOW, together with EDX spectra of the Zn surface in WOW.

O, Zn, and Cl signals were observed in EDX spectra (Figure 2) due to the possible formation of zinc hydroxychloride $[Zn_5(OH)_8Cl_2]$ as a corrosion product on the metal surface.[21] It is generally confirmed that Cl^- ions can interact with Zn^+ and Zn^{++} to form soluble $ZnCl_2^-$, $ZnCl_2$, and β-ZnOHCl, which leads to the formation of $Zn_5(OH)_8Cl_2$ (the main corrosion product of zinc).[22] According to this result, the passive layer formation was successfully inhibited by Cl^- ions, and this leads to continuous generation of H_2 gas till the complete Zn electrode is consumed.

The generation of H_2 gas can occur in the following two ways:[23]

1 Volmer−Tafel way: electroadsorption, followed by chemical combination
2 Volmer−Heyrovsky pathway: electroadsorption, followed by electro-combination.

2.2. Effect of pH and Temperature. A series of experiments were carried out covering a range of pH values between 5.5 and 2.5 to determine the effect of solution pH on hydrogen production efficiency. The impact of solution pH on hydrogen evolution during the dissolution of zinc coupons placed in WOW with time at 298 K is shown in Figure 3a. It is remarkable that pH has a main role to change hydrogen gas production efficiency. Figure 3a shows that low pH enhanced hydrogen production rates and yields. This effect can be interpreted on the basis that the solutions with low pH (less than 7) are considered to be acidic.[1] A lower pH value means there are higher free hydrogen ions, and at the same time, low pH accelerates zinc dissolution by supplying hydrogen ions to the oxidation process.[24]

https://doi.org/10.1021/acsomega.1c04708
ACS Omega 2021, 6, 31964−31970

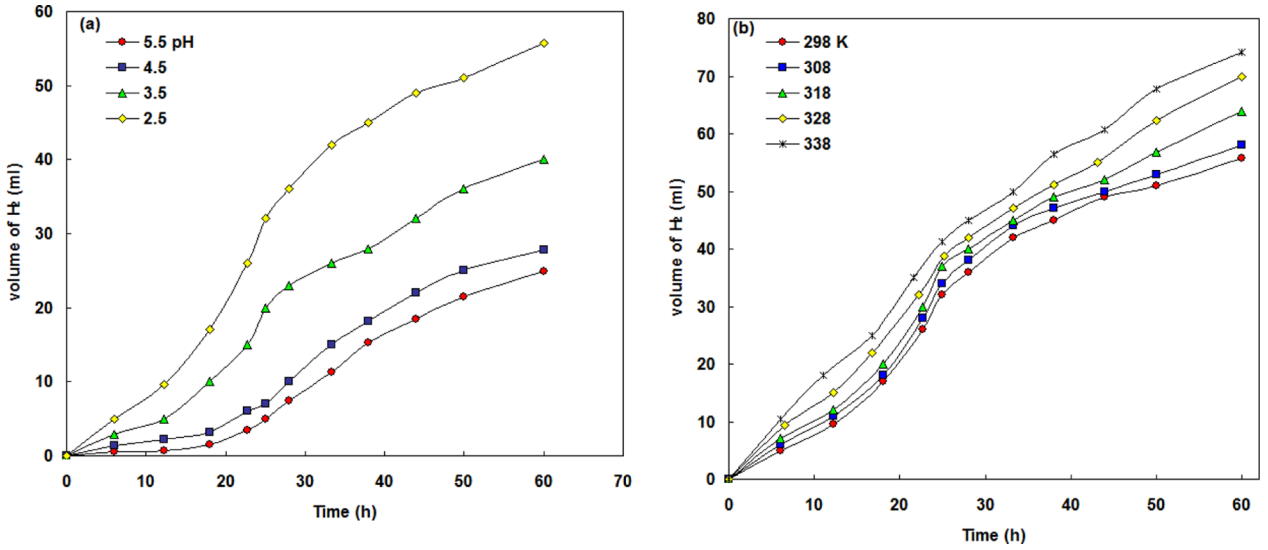

Figure 3. (a) Variation of H_2 volume (mL) with time (h) during the dissolution of the Zn electrode in WOW at different pH values. (b) Variation of the volume of hydrogen gas evolution with time during the corrosion of the Zn electrode in WOW (pH 2.5) at different temperatures.

The effect of temperature on hydrogen production efficiency was inspected through sets of tests at different temperatures. Figure 3b shows the influence of temperature on hydrogen production during the dissolution of zinc in WOW (pH 2.5). As can be observed, an increase in solution temperature from 298 to 338 K caused an increase in hydrogen production. This demeanor is due to the basic rule that is used for controlling the rate of chemical reaction, which states that chemical reaction enhances with increasing temperatures.[25] Increased temperature by 10 °C favors the formation of activated molecules and further increases the reaction rate.[26,27] Moreover, at high temperatures, the protective films on the metals will become weak, and this leads to the susceptibility of the metal dissolution.[28] According to the obtained data from Figure 3b, it is clear that the supplementary temperature input to the WOW allowed to get a higher dissolution rate of zinc and, consequently, higher hydrogen production during the experiments.

To quantify the temperature impact, the Arrhenius equation was used[29]

$$\mathrm{HR} = A \exp(-E_a/RT) \quad (4)$$

where H_R is the hydrogen production rate (H_R was determined from the maximum hydrogen evolution rates obtained at different temperatures, Figure 3b), A is the Arrhenius constant factor, E_a is the apparent activation energy for the hydrogen production process, R is the universal gas constant, and T is the absolute temperature.

The apparent activation energy E_a was determined by linear regression between ln (H_R) and $1/T$ (Figure 4). The linear regression coefficient for relation ln (H_R) and $1/T$ is close to one (R^2 = 0.9726), indicating that the hydrogen production process may be elucidated using the kinetic model.[30] The activation energy of the hydrogen production process was calculated to be 4.28 kJ mol^{-1}. This value indicates that the hydrogen production process is controlled by mass transfer rather than by a chemical step.[31]

2.3. Cathodic Polarization Measurements. To explore the role of solution pH and temperature in hydrogen production and to confirm the abovementioned results, the cathodic polarization behavior of zinc in WOW was studied.

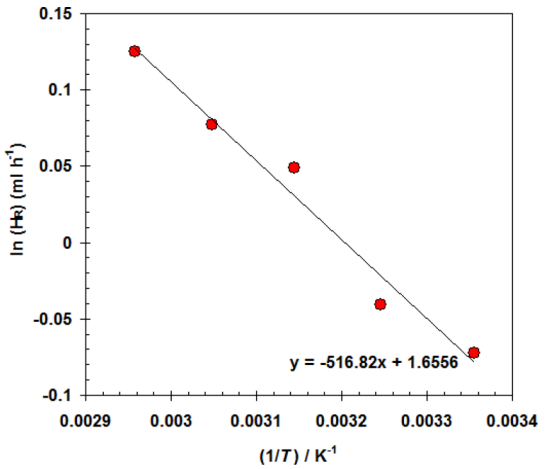

Figure 4. Arrhenius plot for the Zn electrode in WOW (pH 2.5).

Figure 5a shows the cathodic polarization curves for the Zn electrode in WOW at different solution pH values. An important characteristic is that at any polarization potential between −1.15 and −0.9 V, the current is larger at lower pH. On the other hand, Figure 5b shows the cathodic polarization curves for the Zn electrode in WOW (pH 2.5) at different temperatures. It is clear from the figure that at any polarization potential between −1.1 and −0.9 V, the current increases with increasing the temperature. The current is related by Faraday's law to the quantity of the species that is being generated;[30] therefore, an increase in the temperature and a decrease in solution pH cause an improvement in the production rate of H_2 gas.

2.4. Controlling the Hydrogen Generation Reaction by Ionic Liquid. To verify the role of the EMP-ES ionic liquid in the control of hydrogen generation reaction, the rate of hydrogen generation (H_R) and the corresponding efficiency of the EMP-ES ionic liquid (η_{H2} %) during the dissolution of Zn in WOW (conditions: pH 2.5 and 338 K) containing various concentrations of EMP-ES are recoded and listed in Table 1.

η_{H2}% was calculated according to eq 5[32]

https://doi.org/10.1021/acsomega.1c04708
ACS Omega 2021, 6, 31964−31970

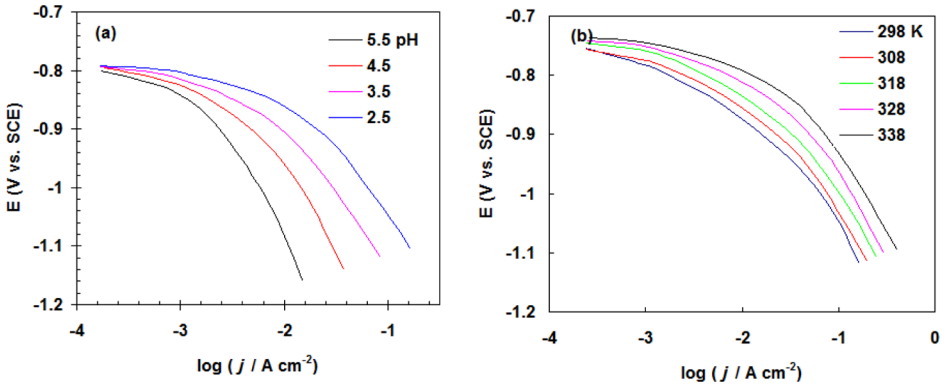

Figure 5. (a) Cathodic polarization curves for the Zn electrode in WOW at different solution pH values. (b) Cathodic polarization curves for the Zn electrode in WOW (pH 2.5) at different temperatures.

Table 1. Rate of Hydrogen Generation (H_R) and the Corresponding Efficiency of the EMP-ES Ionic Liquid (η_{H2} %) During the Dissolution of Zn in WOW at pH 2.5 and 338 K

conc. EMP-ES ppm	H_R (mL h^{-1})	η_{H2} %
WOW	1.2366	
20	0.9153	25.9
40	0.6782	45.1
60	0.3977	67.8
80	0.1243	89.9
100	0.0572	95.3
120	0.0319	97.4

$$\eta_{H2}\% = [(H_R^0 - H_R)/(H_R^0)] \times 100 \quad (5)$$

where H_R^0 represents the rate of hydrogen generation in the blank solution.

Clearly, the rate of hydrogen generation reaction decreases as the concentrations of EMP-ES increase due to the adsorption process on the cathodic sites. It is obvious that η_{H2} % between 25.9% (at 20 ppm) and 97.4% (at 120 ppm) is attributed to the formation of the protective layer of EMP-ES on the Zn surface.[33] The control of the hydrogen generation reaction by the EMP-ES ionic liquid is associated with the adsorption of the negative portion of EMP-ES molecules (i.e., ethyl sulfate) on the Zn surface. This creates partially negative charges on the Zn surface. In this case, the cationic portion of EMP-ES molecules (i.e., 1-ethyl-3-methylpyridinium) screens the negative charge sites of the Zn surface by van der Waals power to prevent the adsorption of H_3O^+. Therefore, the EMP-ES ionic liquid plays a great role in the control of the hydrogen generation reaction.

To further explore the adsorption capability of the EMP-ES ionic liquid on the Zn surface, the Langmuir adsorption isotherm was performed. This isotherm can be represented by the following relations[34]

$$C_{IL}/\theta = (1/K_{ads}) + C_{IL} \quad (6)$$

$$\theta = (H_R^0 - H_R)/(H_R^0) \quad (7)$$

where C_{IL} is the EMP-ES ionic liquid concentration and K_{ads} is the Langmuir isotherm constant.

After a series of isotherms tests, it was found that the Langmuir adsorption isotherm was the best isotherm for the adsorption of the EMP-ES ionic liquid, as shown in Figure 6. This is clear from the value of the correlation coefficient (R^2),

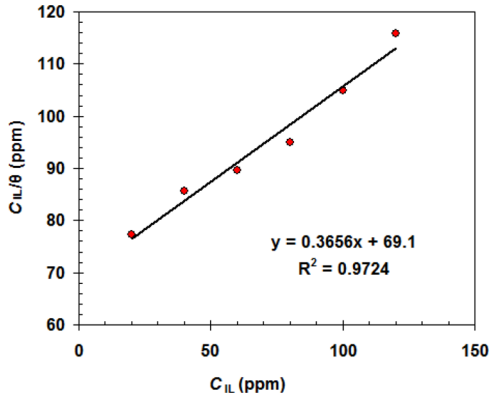

Figure 6. Langmuir adsorption plot for the Zn electrode in WOW containing the EMP-ES ionic liquid.

which is very close to 1 ($R^2 = 0.9724$).[35] Its Langmuir isotherm constant K_{ads} was calculated to be 3.58×10^3 M^{-1}. This high value refers to the strong adsorption of the EMP-ES ionic liquid on the active sites of the Zn surface.[36]

Based on the K_{ads} value, the Gibbs free energy (ΔG°) for the adsorption process can be described as follows[37]

$$\Delta G^\circ = -RT \ln(55.5\, K_{ads}) \quad (8)$$

According to eq 8, ΔG° is -34.22 kJ·mol^{-1}.

This reveals that the adsorption of the EMP-ES ionic liquid on the active sites of the Zn surface is unrestrained with mixing physical and chemical orientations.[38,39]

In order to prove the adsorption of the EMP-ES ionic liquid on the active sites of the Zn surface, FTIR examinations were performed for the pure EMP-ES ionic liquid and the scratched material from the Zn electrode surface (see Figure 7).

The characterized FTIR bands for the pure EMP-ES ionic liquid are clearly observed in Figure 7a. By the interpretation of the FTIR bands for the scratched material from the Zn electrode surface (Figure 7b), it was clear that there are shifts in the C−H (aromatic, Str), C−H (aliphatic, Str), C═C (aromatic, Str), C−N (Str), C−N (Str), C−H out-of-plane bending, and OSO3^{-2} bands. This confirms the adsorption of the EMP-ES ionic liquid on the active sites of the Zn surface.

3. CONCLUSIONS

In this work, the production of H_2 gas has been obtained using the dissolution of zinc metal in WOW at different conditions. The consumed raw materials are only wastewater and zinc.

https://doi.org/10.1021/acsomega.1c04708
ACS Omega 2021, 6, 31964−31970

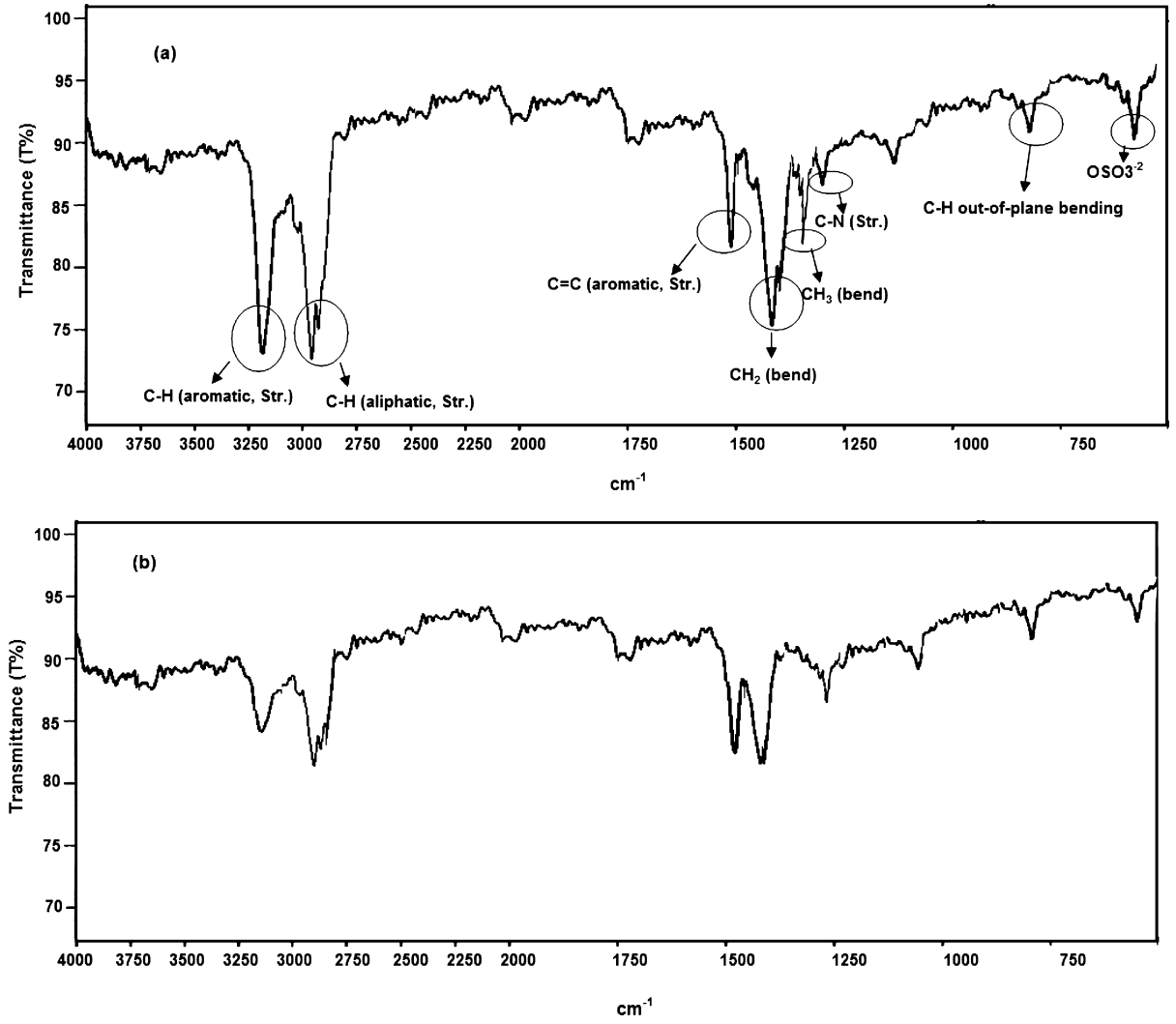

Figure 7. FTIR spectra for (a) pure EMP-ES ionic liquid and (b) scratched material from the Zn electrode surface immersed in WOW containing the EMP-ES ionic liquid.

Therefore, this process represents an economic advantage with respect to hydrogen production using other conventional compounds. The best hydrogen production conditions found were at low pH (2.5) and high temperature (338 K). The EMP-ES ionic liquid plays a great role in the control of the hydrogen generation reaction. The findings of this work can be a building block for the production of pure energy (i.e., hydrogen energy) from waste materials.

4. EXPERIMENTAL SECTION

4.1. Material Preparation. The experiments were carried out using zinc electrodes with composition as follows: Mn (0.005 wt %), Sn (0.070 wt %), Cd (0.520 wt %), Pd (0.18 wt %), Fe (0.035 wt %), and Zn (balance). The surface area of the Zn electrode was close to 4.5 cm^2. The Zn electrode was cleaned with fine grade sandpaper, followed by rinsing with acetone and distilled water and finally dried.

4.2. Chemicals. The test solution used was WOW with the following chemical composition: 67675 ppm Na^+, 2449 ppm Mg^{2+}, 7708 ppm Ca^{2+}, 1272 ppm K^+, 13211 ppm Cl^-, 370 ppm SO_4^{2-}, 600 ppm HCO_3^-, and 568 ppm Br^-. The source of WOW used in the experiment is the Qarun petroleum wells (Egypt).

The pH of WOW was adjusted at 5.5, 4.5, 3.5, and 2.5 by the addition of HCl. The pH of all solutions was measured using a Lseibolo Wien pH meter. The temperature of all test solutions was controlled using a water thermostat (±0.2 °C). EMP-ES 98.0% was purchased from Sigma-Aldrich.

4.3. Hydrogen Evolution Measurements. The device and method for hydrogen gas evolution estimation from the dissolution process have been described elsewhere.[8,17] In a closed vessel, Zn electrodes were dropped into WOW. During the dissolution reaction, the volume of hydrogen gas was evaluated from the change in the level of the paraffin oil in the burette. The variation in the hydrogen gas volume with time was recorded.

4.4. Cathodic Polarization Measurements. For the cathodic potentiodynamic polarization experiments, the standard three-electrode cell (Pt wire as the counter electrode and saturated calomel as the reference electrode and working electrode) was used. The current−potential curves were carried out by changing the potential from −1.15 V to a more positive side with a scan rate of 10 mV s^{-1} until the end of the test. Electrochemical instruments (Gamry reference 3000) with a personal computer were used.

https://doi.org/10.1021/acsomega.1c04708
ACS Omega 2021, 6, 31964−31970

4.5. Surface Analysis. The SEM/EDX analysis for the surface of zinc metal before and after its immersion in WOW was conducted by a scanning electron microscope (JEOL-JEM 1200 EX II) and an energy dispersive spectrometer (Traktor TN-2000).

FTIR examinations were carried out for the pure EMP-ES ionic liquid and the scratched material from the Zn electrode surface by Mattson FTIR Spectrometers (model 960 Mooog).

AUTHOR INFORMATION

Corresponding Author

Mohamed A. Deyab − *Egyptian Petroleum Research Institute (EPRI), Cairo 11251, Egypt;* orcid.org/0000-0002-4053-4942; Phone: +201006137150; Email: hamadadeiab@yahoo.com; Fax: +202 22747433

Author

Ahmed E. Awadallah − *Egyptian Petroleum Research Institute (EPRI), Cairo 11251, Egypt*

Complete contact information is available at: https://pubs.acs.org/10.1021/acsomega.1c04708

Notes

The authors declare no competing financial interest.

ACKNOWLEDGMENTS

The current research was financially supported by the Science, Technology & Innovation Funding Authority, STIFA, Egypt, grant no. 34816.

REFERENCES

(1) Soler, L.; MacAnás, J.; Muñoz, M.; Casado, J. Electrocatalytic Production of Hydrogen Boosted by Organic Pollutants and Visible Light. *Int. J. Hydrogen Energy* **2006**, *31*, 129−139.

(2) Granovskii, M.; Dincer, I.; Rosen, M. A. Exergetic Life Cycle Assessment of Hydrogen Production from Renewables. *J. Power Sources* **2007**, *167*, 461−471.

(3) Eberle, U.; Arnold, G.; Von Helmolt, R. Hydrogen Storage in Metal−Hydrogen Systems and Their Derivatives. *J. Power Sources* **2006**, *154*, 456−460.

(4) Wang, H. Z.; Leung, D. Y. C.; Leung, M. K. H.; Ni, M. A Review on Hydrogen Production Using Aluminum and Aluminum Alloys. *Renew. Sustain. Energy Rev.* **2009**, *13*, 845−853.

(5) Lattin, W. C.; Utgikar, V. P. Transition to Hydrogen Economy in the United States: A 2006 Status Report. *Int. J. Hydrogen Energy* **2007**, *32*, 3230−3237.

(6) Soler, L.; Macanás, J.; Muñoz, M.; Casado, J. Synergistic Hydrogen Generation from Aluminum, Aluminum Alloys and Sodium Borohydride in Aqueous Solutions. *Int. J. Hydrogen Energy* **2007**, *32*, 4702−4710.

(7) Padró, G.; Lau, F. *Advances in Hydrogen Energy*; Padró, G., Lau, F., Eds.; Springer US, 2002.

(8) Deyab, M. A. Effect of Halides Ions on H2 Production during Aluminum Corrosion in Formic Acid and Using Some Inorganic Inhibitors to Control Hydrogen Evolution. *J. Power Sources* **2013**, *242*, 86−90.

(9) Deyab, M. A. Hydrogen Generation during the Corrosion of Carbon Steel in Crotonic Acid and Using Some Organic Surfactants to Control Hydrogen Evolution. *Int. J. Hydrogen Energy* **2013**, *38*, 13511−13519.

(10) Deyab, M. A. Hydrogen Generation by Tin Corrosion in Lactic Acid Solution Promoted by Sodium Perchlorate. *J. Power Sources* **2014**, *268*, 765−770.

(11) Vishnevetsky, I.; Epstein, M. Production of Hydrogen from Solar Zinc in Steam Atmosphere. *Int. J. Hydrogen Energy* **2007**, *32*, 2791−2802.

(12) Soler, L.; Candela, A. M.; Macanás, J.; Muñoz, M.; Casado, J. In Situ Generation of Hydrogen from Water by Aluminum Corrosion in Solutions of Sodium Aluminate. *J. Power Sources* **2009**, *192*, 21−26.

(13) Huang, X.-N.; Lv, C.-J.; Wang, Y.; Shen, H.-Y.; Chen, D.; Huang, Y.-X. Hydrogen Generation from Hydrolysis of Aluminum/Graphite Composites with a Core−Shell Structure. *Int. J. Hydrogen Energy* **2012**, *37*, 7457−7463.

(14) Deyab, M. A. Efficiency of Cationic Surfactant as Microbial Corrosion Inhibitor for Carbon Steel in Oilfield Saline Water. *J. Mol. Liq.* **2018**, *255*, 550−555.

(15) Deyab, M. A.; El Bali, B.; Essehli, R.; Ouarsal, R.; Lachkar, M.; Fuess, H. NaNi(H2PO3)3·H2O as a Novel Corrosion Inhibitor for X70-Steel in Saline Produced Water. *J. Mol. Liq.* **2016**, *216*, 636−640.

(16) Sanatkumar, B. S.; Nayak, J.; Shetty, A. N. Influence of 2-(4-chlorophenyl)-2-oxoethyl benzoate on the hydrogen evolution and corrosion inhibition of 18 Ni 250 grade weld aged maraging steel in 1.0 M sulfuric acid medium. *Int. J. Hydrogen Energy* **2012**, *37*, 9431−9442.

(17) Soler, L.; Macanás, J.; Muñoz, M.; Casado, J. Aluminum and Aluminum Alloys as Sources of Hydrogen for Fuel Cell Applications. *J. Power Sources* **2007**, *169*, 144−149.

(18) El-Sherbini, E. E. F.; Wahaab, S. M. A.; Deyab, M. Ethoxylated Fatty Acids as Inhibitors for the Corrosion of Zinc in Acid Media. *Mater. Chem. Phys.* **2005**, *89*, 183−191.

(19) Holze, R. P. R. R.oberge Corrosion Basics: An Introduction (2nd Ed.). *J. Solid State Electrochem.* **2008**, *12*, 771−772.

(20) Perez, N. *Electrochemistry and Corrosion Science*; Kluwer Academic Publishers: New York, USA, 2004.

(21) Miao, W.; Cole, I. S.; Neufeld, A. K.; Furman, S. Pitting Corrosion of Zn and Zn-Al Coated Steels in PH 2 to 12 NaCl Solutions. *J. Electrochem. Soc.* **2007**, *154*, C7.

(22) Bhardwaj, M.; Balasubramaniam, R. Uncoupled Non-Linear Equations Method for Determining Kinetic Parameters in Case of Hydrogen Evolution Reaction Following Volmer−Heyrovsky−Tafel Mechanism and Volmer−Heyrovsky Mechanism. *Int. J. Hydrogen Energy* **2008**, *33*, 2178−2188.

(23) Roberge, P. R. *59. Corrosion Engineering Principles and Practice*; McGraw-Hill: New York, US, 2008.

(24) Wiersma, B. J.. Hydrogen Generation During the Corrosion of Carbon Steel in Oxalic Acid. **2004**, *00441*, 1−21. DOI: 10.2172/833395

(25) James, O. A.; Akaranta, O. Inhibition of Corrosion of Zinc in Hydrochloric Acid Solution by Red Onion Skin Acetone Extract. *Res. J. Chem. Sci.* **2011**, *1*, 31−37.

(26) Ita, B. I. A. Study of Corrosion Inhibition of Mild Steel in 0.1 M Hydrochloric Acid by o-Vanillin and o-Vanillin Hydrazone | Request PDF. *Bull. Electrochem.* **2004**, *20*, 363−370.

(27) Deyab, M. A. Corrosion Inhibition of Heat Exchanger Tubing Material (Titanium) in MSF Desalination Plants in Acid Cleaning Solution Using Aromatic Nitro Compounds. *Desalination* **2018**, *439*, 73−79.

(28) Peabody, A. W.; Bianchetti, R.; Bianchetti, R. L. *CONTROL OF PIPELINE CORROSION SECOND EDITION | Guru Vasanth*; National Association of Corrosion Engineers, 1967.

(29) Deyab, M. A. Hydrogen Evolution Inhibition by L-Serine at the Negative Electrode of a Lead-Acid Battery. *RSC Adv.* **2015**, *5*, 41365−41371.

(30) Deyab, M. A. Electrochemical Investigations on Pitting Corrosion Inhibition of Mild Steel by Provitamin B5 in Circulating Cooling Water. *Electrochim. Acta* **2016**, *202*, 262−268.

(31) Krishtalik, L. I. *Charge Transfer Reactions in Electrochemical and Chemical Processes*, 1st ed.; Springer US: Consultants Bureau: New York U.S.A., 1986.

(32) Deyab, M. A. 1-Allyl-3-Methylimidazolium Bis-(Trifluoromethylsulfonyl)Imide as an Effective Organic Additive in Aluminum-Air Battery. *Electrochim. Acta* **2017**, *244*, 178−183.

(33) Wang, D.; Zhang, D.; Lee, K.; Gao, L. Performance of AA5052 Alloy Anode in Alkaline Ethylene Glycol Electrolyte with Dicarboxylic

Acids Additives for Aluminium-Air Batteries. *J. Power Sources* **2015**, *297*, 464−471.
(34) John, S.; Jeevana, R.; Aravindakshan, K. K.; Joseph, A. Corrosion Inhibition of Mild Steel by N(4)-Substituted Thiosemicarbazone in Hydrochloric Acid Media. *Egypt. J. Pet.* **2017**, *26*, 405−412.
(35) Li, X.; Deng, S.; Mu, G.; Fu, H.; Yang, F. Inhibition Effect of Nonionic Surfactant on the Corrosion of Cold Rolled Steel in Hydrochloric Acid. *Corros. Sci.* **2008**, *50*, 420−430.
(36) Deng, S.; Li, X. Inhibition by Ginkgo Leaves Extract of the Corrosion of Steel in HCl and H2SO4 Solutions. *Corros. Sci.* **2012**, *55*, 407−415.
(37) Bayol, E.; Gürten, A.; Dursun, M.; Kayakirilmaz, K. Adsorption Behavior and Inhibition Corrosion Effect of Sodium Carboxymethyl Cellulose on Mild Steel in Acidic Medium. *Acta Phys.—Chim. Sin.* **2008**, *24*, 2236−2243.
(38) Avci, G. Inhibitor Effect of N,N′-Methylenediacrylamide on Corrosion Behavior of Mild Steel in 0.5 M HCl. *Mater. Chem. Phys.* **2008**, *112*, 234−238.
(39) Ashassi-Sorkhabi, H.; Shaabani, B.; Seifzadeh, D. Corrosion Inhibition of Mild Steel by Some Schiff Base Compounds in Hydrochloric Acid. *Appl. Surf. Sci.* **2005**, *239*, 154−164.

https://doi.org/10.1021/acsomega.1c04708
ACS Omega 2021, 6, 31964−31970